Scientific Research Publishing

International Journal of Geosciences, 2024, 15, 525-548
https://www.scirp.org/journal/ijg
ISSN Online: 2156-8367
ISSN Print: 2156-8359

Obtaining 2D Soil Geotechnical Profiles from Cokriging Interpolation of Sample Data and Electrical Resistivity Tomography (ERT)—Applications in Mass Movements Studies

Cassiano Antonio Bortolozo[1,2*], Noel Howley[3], Andy Legg[4], Tristan Pryer[3,4], Danielle Silva de Paula[2], Tatiana Sussel Gonçalves Mendes[1], Daniel Metodiev[1,2], Marcio Roberto Magalhães de Andrade[2], Silvio Jorge Coelho Simões[1], Maiconn Vinicius de Moraes[1], Marcio Augusto Ernesto de Moraes[2], Luana Albertani Pampuch[1], Rodolfo Moreda Mendes[2], Harideva Marturano Egas[1,2]

[1]Institute of Science and Technology, São Paulo State University (UNESP), São José dos Campos, Brazil
[2]Cemaden-National Center for Monitoring and Early Warning of Natural Disasters, General Coordination of Research and Development, São José dos Campos, Brazil
[3]Institute for Mathematical Innovation, University of Bath, Bath, UK
[4]Department of Mathematical Sciences, University of Bath, Bath, UK
Email: *cassianoab@gmail.com

How to cite this paper: Bortolozo, C.A., Howley, N., Legg, A., Pryer, T., de Paula, D.S., Mendes, T.S.G., Metodiev, D., de Andrade, M.R.M., Simões, S.J.C., de Moraes, M.V., de Moraes, M.A.E., Pampuch, L.A., Mendes, R.M. and Egas, H.M. (2024) Obtaining 2D Soil Geotechnical Profiles from Cokriging Interpolation of Sample Data and Electrical Resistivity Tomography (ERT)—Applications in Mass Movements Studies. *International Journal of Geosciences*, **15**, 525-548.
https://doi.org/10.4236/ijg.2024.157029

Received: July 2, 2024
Accepted: July 19, 2024
Published: July 22, 2024

Abstract

Brazil annually faces significant challenges with mass movements, particularly in areas with poorly constructed housing, inadequate engineering, and lacking sanitation infrastructure. Campos do Jordão, in São Paulo state, is a city currently grappling with these issues. This paper details a study conducted within a pilot area in Campos do Jordão, where geophysical surveys and geotechnical borehole data were integrated. The geophysical surveys provided 2D profiles, and samples were collected to analyse soil moisture and plasticity. These datasets were combined using a Cokriging-based model to produce an accurate representation of the subsurface conditions. The enhanced modelling of subsurface variability facilitates a deeper understanding of soil behavior, which can be used to improve landslide risk assessments. This approach is innovative, particularly within the international context where similar studies often do not address the complexities associated with urban planning deficits such as those observed in some areas of Brazil. These conditions, including the lack of proper sanitation and irregular housing, significantly influence the geological stability of the region, adding layers of

complexity to subsurface assessments. Adapting geotechnical evaluation methods to local challenges offers the potential to increase the efficacy and relevance of geological risk management in regions with similar socio-economic and urban characteristics.

Keywords

Mass Movements, Geophysics, ERT, Geotechnical Surveys, Campos do Jordão, Cokriging

1. Introduction

Landslides are complex geological phenomena influenced by a variety of interrelated factors that can be broadly categorized into geological, morphological, physical, human, and climatic influences. Geological factors, such as the type and structure of rock and soil, play a crucial role, with certain materials like clay-rich soils and weathered rocks being more prone to landslides due to their weak structural properties. Morphological factors, including slope gradient and shape, significantly impact susceptibility, as steeper and convex slopes are generally more prone to instability. Physical factors, particularly water content, greatly affect slope stability; increased soil moisture from rainfall can raise pore pressure and reduce cohesion between soil particles, leading to landslides. Vegetation cover can stabilize slopes, while deforestation increases risk. Human activities, such as deforestation, mining, and infrastructure development, often destabilize slopes by altering natural drainage patterns and removing stabilizing vegetation. Climatic factors, especially intense or prolonged rainfall, act as major triggers for landslides by increasing soil moisture content and reducing soil strength, while temperature fluctuations can weaken rock and soil structures. Effective landslide management requires a comprehensive understanding of these factors, integrated risk assessment approaches, and sustainable land use practices to mitigate adverse impacts on human lives and infrastructure.

The recent report by the Intergovernmental Panel on Climate Change (IPCC) of the United Nations, published in August 2021, highlights the escalating intensity and frequency of extreme weather and climate events due to climate change [1]. This increase in extreme events, coupled with societal factors, is likely to lead to more frequent natural disasters [2]. Specifically, the IPCC report forecasts an increase in precipitation in the northwest and southeast regions of Brazil, potentially exacerbating the incidence of floods, droughts, and landslides—already the most common natural disasters in these areas [1].

Urban landslides, in particular, have shown a consistent annual increase, primarily due to unregulated urban expansion and the settlement of high-risk areas by economically disadvantaged groups. The Brazilian Institute of Geography and Statistics (IBGE) reports that, from 2009 to 2013, there were 30,858 instances of mass movements affecting 895 municipalities. Notably, the southern, southeas-

tern, and northeastern regions of Brazil are most prone to landslides. In the southeastern and northeastern regions, 27,940 landslides were recorded during the same period, with the states of Pernambuco (5910), São Paulo (4981), and Rio de Janeiro (4,969) accounting for more than half of these events [3].

The gravest landslide incidents have led to significant fatalities and substantial material damages, profoundly affecting local populations. A study by the Federal University of Santa Catarina's Center for Natural Disaster Monitoring and Early Warning [4] reports that landslides resulted in 1403 deaths in Brazil between 1991 and 2010, impacting 173,259 people. Reference [5] notes a high fatality rate from landslides, with an average of approximately two deaths per event. The 2011 landslide disaster in the mountainous region of Rio de Janeiro state stands out as the most devastating, with 830 fatalities and nearly 9,988 individuals displaced [6].

Landslide occurrences in Brazil, as in many other global regions, are frequently linked to rainfall events [7]-[9]. Nonetheless, the distribution of geological structures and the properties of subsurface layers also significantly influence landslide dynamics. This complex interplay complicates the monitoring and understanding of mass movements, as the processes leading to landslides are intricate and depend on multiple variables [10].

The challenges posed by landslides underscore the necessity for a comprehensive and multidisciplinary approach to hazard assessment and mitigation. Researchers are actively working to improve early warning systems and disaster preparedness strategies [11]-[13]. In geotechnical research, traditional methods often focus on direct investigation techniques, which include borehole drilling, the extraction of both undisturbed and disturbed soil samples, and the conduction of field and laboratory tests. These techniques generally involve localized assessments at varying depths to determine critical soil parameters.

To develop a more nuanced understanding of the dynamics underlying mass movements, indirect methodologies such as geophysical investigations are employed. These methods provide a spatial representation of subsurface conditions and can be integrated with direct approaches to refine estimates of essential soil parameters [14] [15]. Studies by [16]-[20] have demonstrated the utility of geophysical testing in enhancing the interpretation of geological and geotechnical profiles related to mass movements. Collectively, these integrated methodologies enable a precise delineation of instability zones [21] [22].

Electrical Resistivity Tomography (ERT) is employed to indirectly derive geotechnical parameters from electrical resistivity data. The software "Guara" [23] computes a range of geotechnical parameters based on a geoelectrical model, utilizing formulas from [24] and [25]. Predominantly, these parameters are derived using formulas established by [24] and are applicable to three soil scenarios: all soil types (general formula), sandy soil, and silt-sand soil. The parameters calculated through this method include density, cohesion, friction angle, soil moisture, plasticity, and hydraulic conductivity. Reference [26] provides an

analysis of the results generated by this software. It is important to note, however, that the models obtained via this indirect approach do not integrate direct data from samples collected at the geophysical survey sites.

Additionally, the research by [27] explores the use of Kriging and Cokriging techniques to produce soil moisture maps by combining data from soil samples and electrical surveys. Kriging, a widely used regression algorithm in geostatistics, estimates unknown parameter values by linearly combining data from adjacent locations [28]. Cokriging, a multivariate extension of Kriging, estimates one parameter based on other known parameters, allowing for a vector of values at each sampled location. In their study, [27] utilizes a Cokriging algorithm to interpolate soil moisture data, using soil sample data and electrical resistivity models from electrical surveys as interpolative guides.

The current project develops a methodology that employs a similar approach, using parameters derived indirectly through the "Guara" software [23]. This methodology utilizes Cokriging to process geotechnical parameter profiles, specifically soil moisture and the plasticity index, derived from the electrical resistivity profile as primary data. Measurements from soil samples along the profile serve as secondary data. This Cokriging approach integrates the primary, indirectly obtained geophysical data with localized geotechnical data, providing a comprehensive and reliable representation of soil parameters. Such advancements are crucial for enhancing the understanding of mass movement processes and augmenting the resource base of the Cemaden Operational Room staff responsible for monitoring slopes. This project is particularly focused on Campos do Jordão, identified as a critical region with accessible geotechnical data.

2. Study Area

Campos do Jordão, situated in the Mantiqueira Mountains at an elevation of 1628 meters above sea level, is widely recognized as a prominent winter tourist destination, earning the moniker "Brazilian Switzerland." Despite its appeal, the city has experienced significant mass movement incidents, which have been extensive [29] [30]. Urban expansion into steep slope areas, often through irregular settlements, has heightened the risks associated with these mass movements [31]. **Figure 1** illustrates the significant impact of landslides on local communities.

In response, Campos do Jordão has established a comprehensive mass movement monitoring network and boasts a well-trained Civil Defence team. The historical records of mass movements, coupled with data from geotechnical sensors, render the city an exemplary site for studying the integration of geophysical methods with geotechnical data.

The specific region selected for this study, as depicted in **Figure 2**, is situated within a facility operated by the São Paulo State Basic Sanitation Company (SABESP). SABESP is a mixed-capital entity responsible for water supply, as well as the collection and treatment of sewage across 375 municipalities in São Paulo state. The data collection for this research was conducted at a SABESP unit located

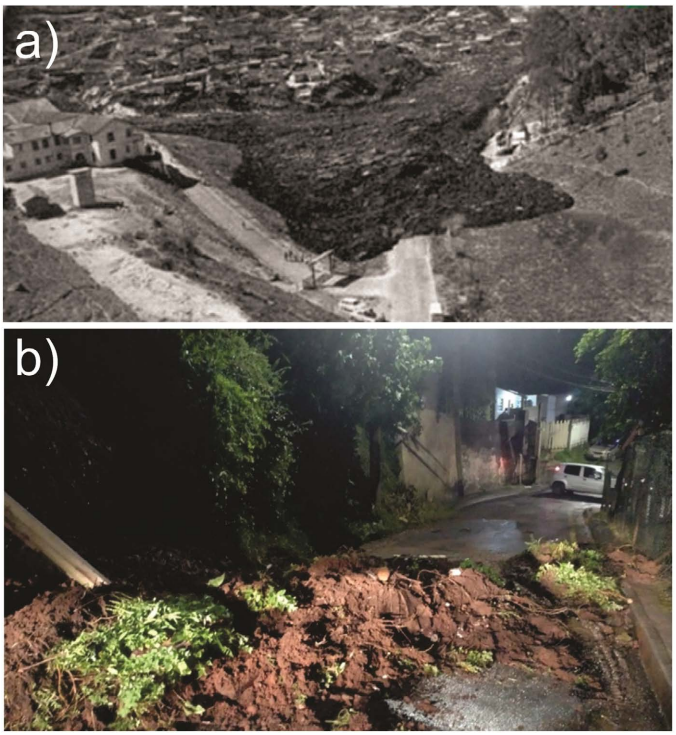

Figure 1. Mass movement events in Campos do Jordão. In (a) the Mudflow in Vila Albertina neighborhood in 1972 (source: O Estado de São Paulo journal) and in (b) the most recent landslide occurred in 2023 also in Vila Albertina neighborhood (source: Campos do Jordão Civil Defense).

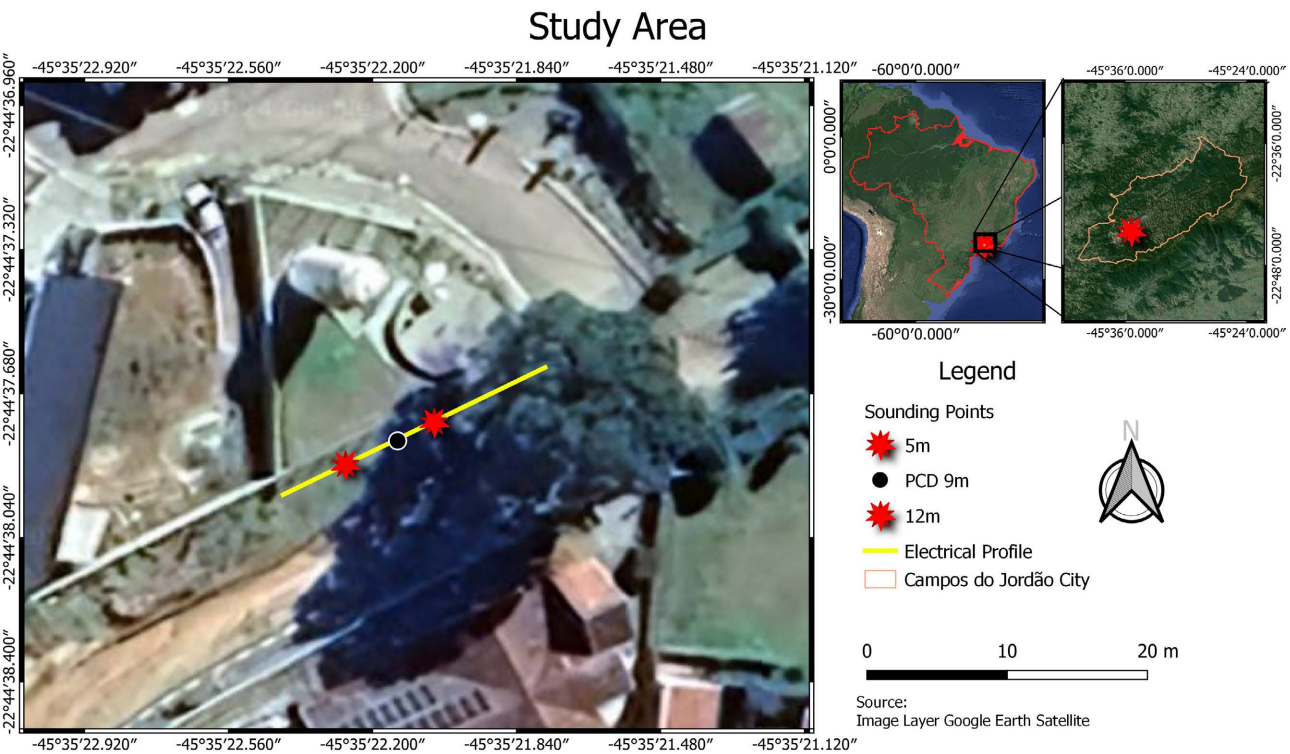

Figure 2. The city of Campos do Jordão, is located in the Mantiqueira Mountain at 1,628 meters above sea level, latitude 22˚44'20"S and longitude 45˚35'27"W.

on a hilltop within an urban area of Campos do Jordão, offering environmental characteristics representative of the wider municipality. In the study area, samples were collected along the electrical resistivity profile at positions 5 m and 12 m (Figure 2). At each of these positions, 6 samples were collected, ranging from 0.25 m to 2.6 m depth.

3. Local Geology

Campos do Jordão is located within the Atlantic Shield, specifically in the Mantiqueira Geotectonic Province, which was influenced by the Brasiliana Orogeny, dating from 670 Ma to 550 Ma, on the South American plate. This area is characterized by a diverse array of geological structures, notably including the Buquira reverse dextral shear zone [32]-[34]. The city is strategically positioned in a transitional zone among several tectonostratigraphic units: the Apiaí-Guaxupé Terrain (Socorro-Guaxupé Nappe), the Embu Terrain, and the Taubaté Basin, which is part of the Southeastern Brazil continental rift system [35] dating back to the Tertiary period.

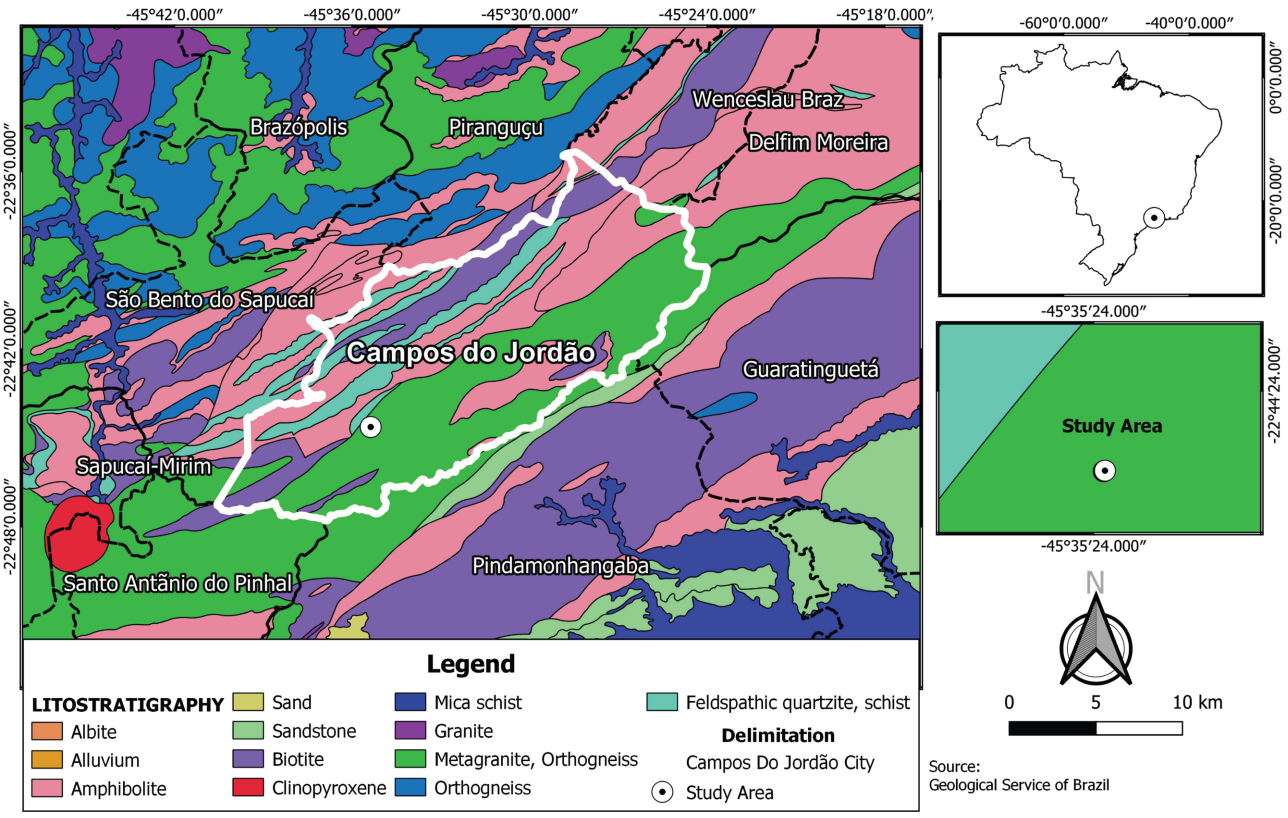

Figure 3. Map and local geology of Campos do Jordão in the Mantiqueira Mountains.

As illustrated in Figure 3, the regional lithological map showcases a predominance of orthogneisses (migmatitic) from the Varginha-Guaxupé Complex, along with amphibolite and sandstone, which form the foundational geological layer of the study area. In the southeastern section of the map, a belt extends

from southwest to northeast, composed primarily of schists (biotite schist) and gneisses (biotite granitic gneiss, migmatite gneiss) from the Embu Complex. The Varginha-Guaxupé and Embu complexes have been intruded by several granite bodies, indicative of the metaluminous magmatism associated with the Neoproterozoic orogeny. In a narrow central-southern portion of the region, Paleozoic metasediments are evident, linked to sedimentation in an extensional basin that predated the primary collision event responsible for the formation of the Mantiqueira Province. Within the Brazilian Southeast Rift, the region also hosts conglomerates, sandstones, and shales from fluvial and lacustrine environments, which are components of the Taubaté Group deposited during the Paleogene and Neogene periods.

The maturity of residual soils and deeply weathered rock in the study area suggests a history of a wet, warm climate over millions of years, leading to extensive Quaternary pedological and sedimentary coverage. The geomorphological conditions, including fluvial sedimentation confined to erosive channels in narrow, incised valleys, indicate morphogenesis associated with a recent epigenetic cycle. This environment, where soil saturation creates a reducing and acidic milieu, facilitates the chemical weathering of migmatite gneiss minerals, resulting in the formation of gray hydromorphic soils (Gleisols).

The geological substrate comprises a variety of rock types from hornblende-biotite to biotite orthogneisses with granodioritic to tonalitic compositions, all exhibiting migmatitic features and stromatic textures with interspersed amphibolite lenses [36]. Within the soil profiles, silty sand and clayey silt are observed, outcomes of differentiated weathering processes acting on the felsic (sand) and amphibolitic (clay) minerals derived from the granodiorites and tonalites.

These geological conditions, especially the presence of deeply weathered and structurally complex migmatites and gneisses, are particularly significant in assessing landslide risks. The pronounced weathering and structural heterogeneity of these rock types often lead to differential erosion and mechanical weakening, which are critical factors in landslide initiation. Moreover, the hydrogeological conditions are critical for landslide susceptibility by promoting water saturation and subsequent soil instability [37]. Therefore, understanding these specific geological formations provides crucial insights into the inherent landslide risks within the region, informing both hazard assessment and mitigation strategies.

4. Geophysical Method - Electrical Resistivity

The electrical resistivity (ER) method primarily aims to map the distribution of electrical resistivity in the subsurface. This technique is extensively employed worldwide, including in Brazil, across various domains such as academic research and commercial applications. Its versatility allows for its use in diverse fields, including groundwater exploration [38]-[42], mineral prospecting, archaeological surveys, environmental studies, geothermal resource identification, and engineering geology [43]. Notably, the ER method is a cornerstone geo-

physical technique in the analysis of mass movements, as evidenced by studies conducted by [44]-[48].

The operational mechanism of the ER method involves the injection of an electric current into the ground using two electrodes, known as current electrodes, which may be positioned on the surface or within boreholes. The electric potential created by this current is measured using a separate pair of electrodes, referred to as potential electrodes. The spatial arrangement of these electrodes is crucial as it facilitates the estimation of electric resistivity values. According to [49], the apparent electrical resistivity, denoted ρ_a, can be calculated through

$$\rho_a = K\frac{\Delta V}{I} \tag{1}$$

where K represents the geometric factor, which is contingent upon the spatial arrangement of the electrodes. The potential difference, ΔV, measured between the potential electrodes M and N, and I, the current injected into the ground through the current electrodes A and B.

With recent advancements in geophysical equipment, such as the introduction of smart electrode systems, the efficiency and data quality of surveys have significantly improved. These smart electrodes automate many of the traditional manual adjustments and can be deployed rapidly, allowing for extensive data sampling over shorter periods. This technological evolution not only speeds up the survey process but also enhances the spatial resolution and depth of data acquisition, facilitating a more detailed and accurate geological assessment.

The Electrical Resistivity Profile (ERT) carried out in this work covered a span of 17.75 meters, employing a dipole-dipole array configuration. This array was equipped with 72 smart electrodes spaced at 0.25 meters, and the data acquisition was conducted using a Syscal Pro resistivity meter. Data inversion processes were carried out utilizing the Res2DInv software developed by Seequent.

5. Results

5.1. Sampling

In the study area, samples were collected along the electrical resistivity profile at positions 5 m and 12 m, as indicated in **Figure 2**. At each position, six samples were collected at depths ranging from 0.25 m to 2.6 m. In this study, we chose to employ the parameters of soil moisture and plasticity index due to their frequent analysis in laboratory environments and their significant relevance in landslide studies. Increasing soil moisture from rainfall can raise pore pressure and reduce cohesion between soil particles, leading to landslides. Furthermore, the soil's plasticity index is another important parameter in assessing landslide studies. The plasticity index represents the amount of water necessary to transition a soil from its plastic state to its liquid state, indicating the soil's capacity to undergo deformation before failure. The Cokriging methodology utilized the resistivity profile, obtained through electrical inversion, as the basis for indirect calculations of soil moisture and the plasticity index. These calculations serve as pri-

mary data for integrating geophysical and geotechnical properties.

The 12 soil samples were processed to determine their moisture content and plasticity index values, which are displayed in Table 1. This data constituted the secondary dataset. Subsequently, Cokriging interpolation was employed to refine the accuracy of the profiles derived from the resistivity model. As a validation step, the new soil moisture model, resulting from the integration of indirect data with sample measurements, was compared to the values measured by the Soil Moisture Sensors of the Data Collection Platform (PCD) Station [50], located at the midpoint (9 m) of the profile. This comparison helps validate the effectiveness of the cokriging method in predicting soil conditions based on geophysical data.

This approach not only enhances the precision of geotechnical assessments but also provides a robust framework for understanding subsurface properties in environments prone to natural disturbances such as landslides.

Table 1. Soil moisture values and plasticity index for the collected samples.

Sample	Sampled depth (m)	Moisture (%)	Plasticity index (%)
CE1_5m	0.25 - 0.6	31.4	14
	0.6 - 0.9	33.4	11
	1.0 - 1.4	39.2	10
	1.4 - 1.8	47.1	7
	1.8 - 2.2	46.5	9
	2.2 - 2.6	53.6	8
CE1_12m	0.2 - 0.6	23.2	8
	0.6 - 1.0	26.1	14
	1.0 - 1.4	47.5	17
	1.4 - 1.8	47.1	19
	1.8 - 2.2	46.2	22
	2.2 - 2.6	44.2	10

5.2. Cokriging Algorithm

The accuracy of the cokriging methodology is influenced by various interrelated factors that must be carefully considered and optimized to ensure reliable spatial interpolation and geostatistical analyses. One primary factor is the spatial correlation structures of both the primary and secondary variables. High spatial correlation within the primary variable often results in more accurate predictions, and a well-correlated secondary variable is equally crucial. The quality and quantity of data significantly impact cokriging accuracy. Data density, or the number of sampling points for both primary and secondary variables, plays a critical role; generally, a higher density of data points leads to more precise estimates. Furthermore, the quality of the input data, including the precision and

accuracy of measurements, directly affects the output of cokriging. The choice and modeling of the cross-variogram are critical components. Selecting an appropriate variogram model, such as spherical, exponential, or Gaussian (as used in this work), and accurately determining its parameters, often through trial and error, are essential for achieving reliable results.

In addressing the problem, primary and secondary data are defined as $Z_1(x)$ and $Z_2(x)$, respectively. The objective in Cokriging is to estimate $Z(x)$, which represents the predicted value at a location x. The weights for the primary and secondary datasets, λ_{1i} and λ_{2j}, are determined based on a variogram model, which quantifies the spatial variability and correlation structure of a spatial variable. The estimation of Z(x) is then given by a linear combination of the two datasets

$$Z(x) = \sum_{i=1}^{n_1} \lambda_{1i} Z_1(x_i) + \sum_{j=1}^{n_2} \lambda_{2j} Z_2(x_j). \quad (2)$$

The standard semivariogram, $\gamma(h)$, measures the degree of spatial dependence between sample points separated by distance h and is typically defined as

$$\gamma(h) = \frac{1}{2}\mathbb{E}\left[\left(Z(x+h) - Z(x)\right)^2\right]. \quad (3)$$

Here, $\mathbb{E}$ represents the expectation operator. Given the limited number of secondary data points (approximately 12 in this study), it is challenging to compute a reliable cross-variogram directly. We have used a Gaussian distribution for the semivariogram motivated in capturing long-range dependencies and providing a smoother representation of the underlying spatial continuity. The Gaussian semivariogram is

$$\gamma(h) = e^{\frac{-|h|^2}{\theta^2}}, \quad (4)$$

where θ is the correlation range.

5.3. Cokriging Interpolation - ERT Profile and Soil Moisture

Table 2 provides a breakdown of the granulometry derived from soil samples collected during this project, including those obtained during the installation of the PCD at the 9 m mark on the geophysical profile. The granular composition at the 5 m and 9 m positions indicates a predominance of silt, with the initial two samples at 5 m being mainly clayey. Notably, the sample from a depth of 2.6 m at the 9 m mark shows a higher sand content (41%) compared to silt (37%). At the 12 m position, the top sample contains 43% sand, while the subsequent samples primarily consist of clay, with the exception of samples 3 and 4, which display almost equal proportions of clay and silt. The final sample at this position is primarily silty.

The inverted ERT model, illustrated in Figure 4(a), exhibits complex two-dimensional features with significant resistivity variations across the surveyed area. Notably, the majority of these anomalies are more indicative of anthropogenic interferences rather than natural variations in soil composition

(Figure 4(b)). The prevalence of such anomalies can largely be attributed to recent urban developments in the survey area, which underwent extensive modifications less than a year prior to the survey in May 2023. These modifications included substantial roadworks and the installation of multiple pipelines from the water distribution station, all of which contributed to notable alterations in the subsurface profile.

Table 2. Granulometry from the samples acquired in this research (positions 5 m and 12 m) and from the samples acquired during the PCD Geo installation.

Sample	Sampled depth (m)	Granulometry (%)						
		Gravel	Coarse sand	Medium sand	Fine sand	Total sand	Silt	Clay
ERT_5m_1	0.25 - 0.6	0	1	14	18	33	27	40
ERT_5m_2	0.6 - 0.9	0	4	12	20	36	27	37
ERT_5m_3	1.0 - 1.4	0	4	10	16	30	46	24
ERT_5m_4	1.4 - 1.8	0	7	15	20	42	49	10
ERT_5m_5	1.8 - 2.2	0	6	12	18	36	48	17
ERT_5m_6	2.2 - 2.6	0	3	11	21	35	51	14
ERT_9m_1	0.2 - 0.7	0	5	10	14	29	41	30
ERT_9m_2	0.7 - 1.4	0	6	13	18	37	53	10
ERT_9m_3	1.4 - 1.9	0	2	6	11	19	60	21
ERT_9m_4	1.9 - 2.4	0	3	6	14	23	59	18
ERT_9m_5	2.4 - 2.9	0	2	15	24	41	37	22
ERT_9m_6	2.9 - 3.5	0	1	4	12	17	53	30
ERT_12m_1	0.2 - 0.6	0	4	16	23	43	37	21
ERT_12m_2	0.6 - 1.0	0	4	11	18	33	23	43
ERT_12m_3	1.0 - 1.4	0	2	6	13	21	39	40
ERT_12m_4	1.4 - 1.8	0	1	5	14	20	39	41
ERT_12m_5	1.8 - 2.2	0	2	5	14	21	35	45
ERT_12m_6	2.2 - 2.6	0	1	5	12	18	48	34

At position $x = 5$ m and $y = 0.27$ m, a high resistivity value exceeding 10,000 Ohm.m suggests the presence of a pipeline. Similarly, other areas near a depth of 0.5 m, which display high resistivity, are likely associated with buried debris or pipelines. These resistive anomalies occur because construction activities often involve the mixing of debris with the soil, leaving it uncompacted. Consequently, materials such as concrete, which are resistive in nature, mix into the relatively porous soil containing air-filled voids, thereby increasing the resistivity observed in the ERT data.

Additionally, it is plausible that some of the high-resistivity anomalies exceeding 7000 Ohm.m could be attributed to smaller pipelines leading to the water reservoir, although this hypothesis could not be definitively confirmed with

the available data.

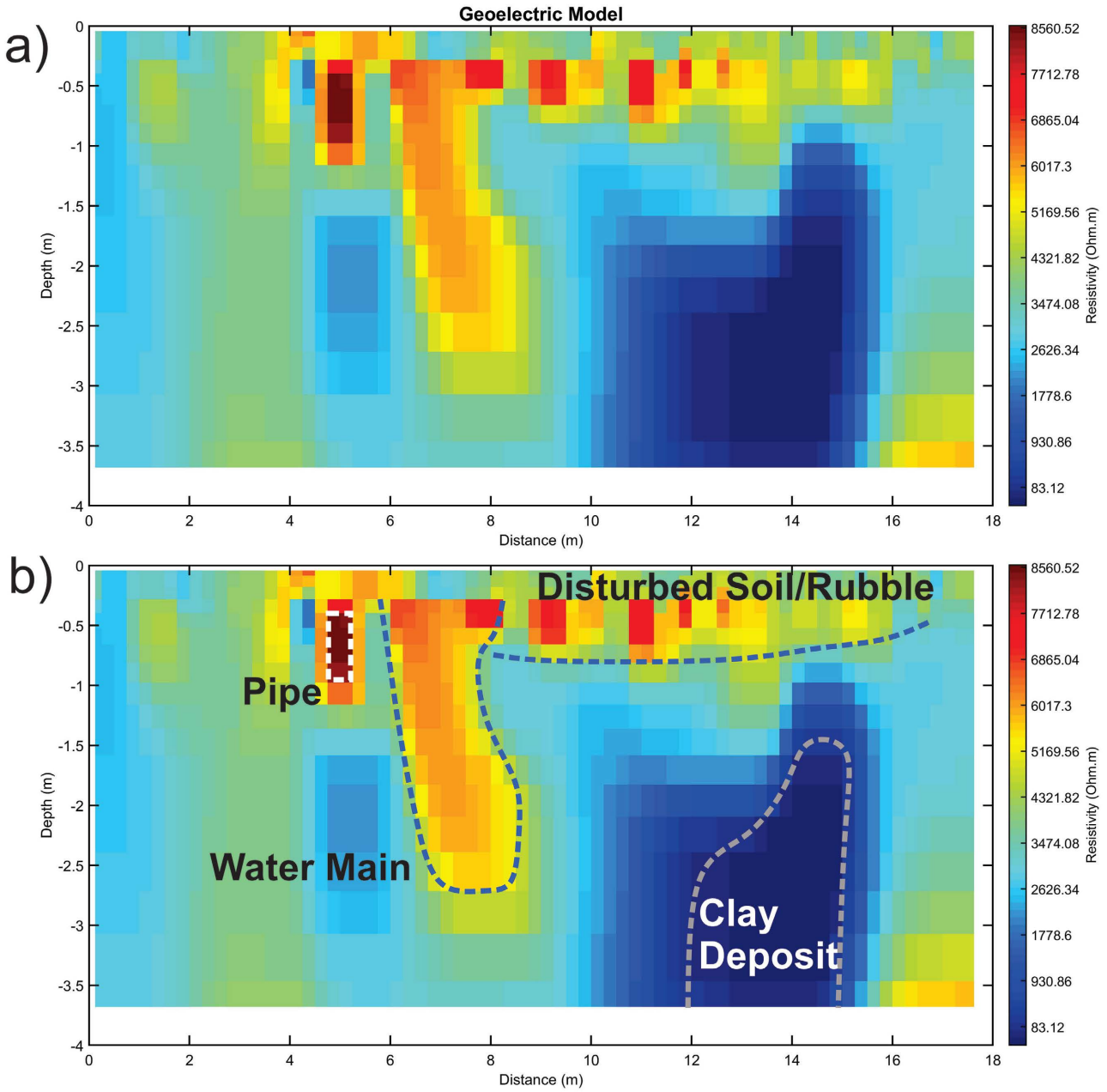

Figure 4. Geoelectric Model. In (a) inverted model used to indirectly calculate soil moisture and plasticity index. In (b) interpretation of detected anomalies.

The ERT survey detected a high resistivity anomaly spanning from a depth of 0.25 m to 2.75 m between positions $x = 7$ m to $x = 8$ m. This anomaly correlates with the presence of a concrete access manhole to a water main located approximately 7 m from the survey line, suggesting its association with the water main. The installation of this infrastructure, typically requiring trench excavation, likely influenced the subsurface resistivity pattern observed. Additionally, the anomaly at the $x = 9$ m position, with a depth of approximately 2.7 m, shows an

increased sand concentration, further linking it to the disturbances from the water main installation.

Beginning at $x = 4.5$ m and a depth of 1.5 m, another notable anomaly extends to the end of the profile. This feature, characterized by larger silt portions as indicated by sample results, sees its lateral continuity disrupted by the water main. A distinct conductive anomaly is present from positions $x = 12$ m to $x = 15$ m at about 1.5 m depth, likely reflecting a higher clay concentration, which increases further below 2.5 m.

Figure 5 displays the soil moisture profile derived indirectly from the electrical resistivity data using formulas from [24]. This profile forms the primary data for the subsequent Cokriging analysis. The site has experienced considerable anthropogenic modifications, which potentially compromise the accuracy of indirect moisture content estimations, particularly in regions with extensive alterations or the presence of structures like pipelines. Notably, extremely low moisture values detected in areas with pipelines and debris, as seen in Figure 4, highlight the limitations of indirect measurements in heavily altered zones.

The use of Cokriging in this context is very useful as it integrates both indirect and direct sample data, enhancing the precision of the two-dimensional moisture model and mitigating the influence of anthropogenic structures.

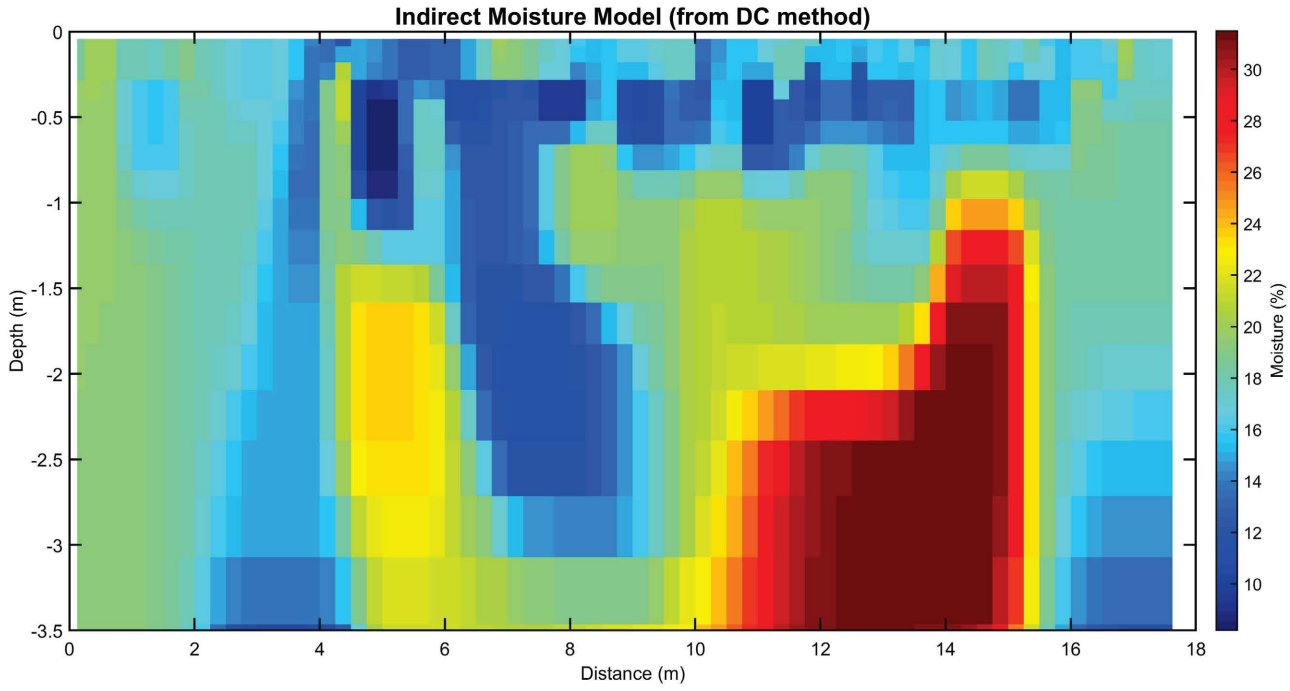

Figure 5. Primary data for soil moisture Cokriging. Soil moisture model was obtained indirectly from the resistivity model.

Figure 6 shows the model resulting from the integration of moisture data derived from the samples listed in Table 1 as secondary data. This model combines both indirect data from electrical resistivity profiles and direct measurements from soil samples. The integrated model exhibits significantly fewer instances of

near-zero moisture values, which predominantly occur around the 0.5 meters depth due to the presence of pipes and related anomalies identified in the primary model.

Notice the diminished correlation with anthropogenic anomalies, highlighting the integrated approach's ability to discriminate between natural soil characteristics and disturbances caused by human activities. Additionally, the model's variations are not confined to the direct sample locations; they extend across the whole surveyed area.

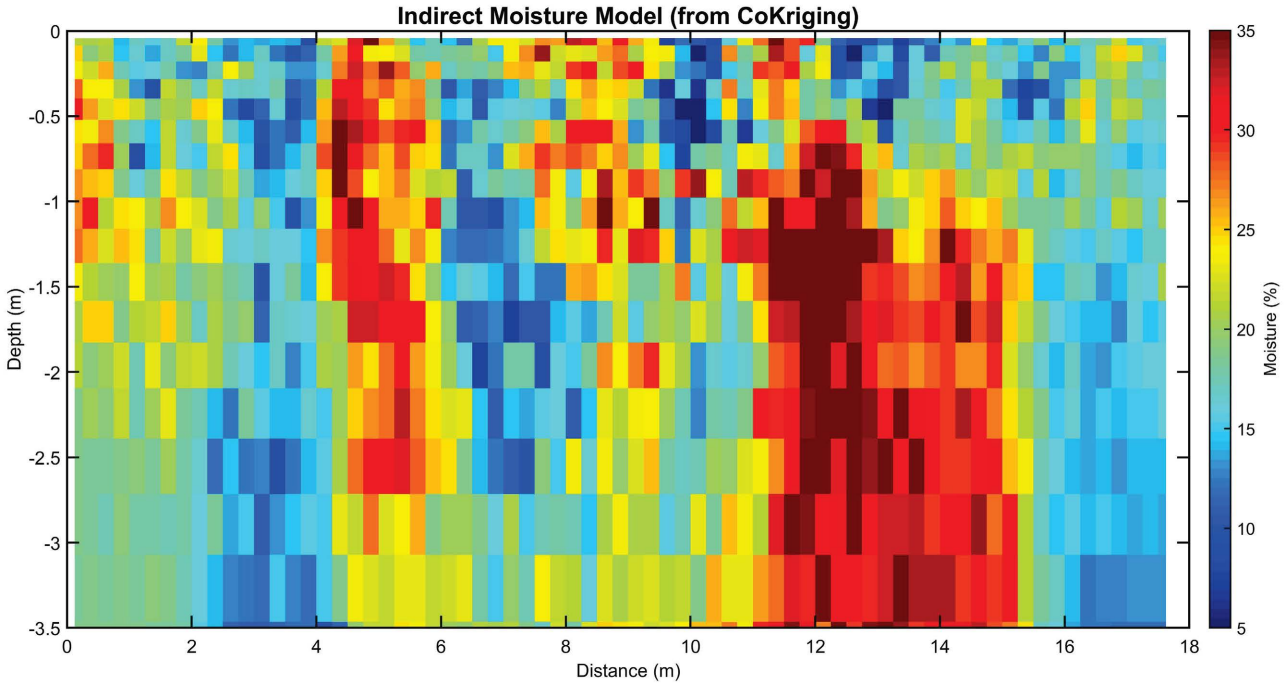

Figure 6. Soil moisture model obtained with the CoKriging algorithm.

Figure 7 illustrates the disparities between the moisture model obtained indirectly from the electrical resistivity profile and the final model refined through Cokriging. The comparison reveals significant discrepancies primarily around the sample locations, although the variations extend beyond these specific points. The most pronounced changes are observed at certain depths at the sample collection sites, with the greatest deviation—approximately 20%—occurring near the pipeline at position $x = 5$ m/$y = 0.75$ m.

The model is globally influenced, indicating adjustments in areas even without direct nearby samples. For instance, the region identified as the water main around position $x = 8$ m/$y = 2$ m shows a considerable variation of about 10%.

In Figure 8(a), a comparison is provided between moisture values obtained from direct sampling, the indirect method via the electrical resistivity profile, and the Cokriging approach at the 5 m position along the geophysical profile. Similarly, Figure 8(b) shows the comparison for the 12 m position. The moisture values derived from the primary model do not closely align with those obtained from direct sampling. This discrepancy can be attributed to the extensive

alterations and recent material displacements in the survey area, which likely compromised the accuracy of the moisture values calculated using [24]'s formulas.

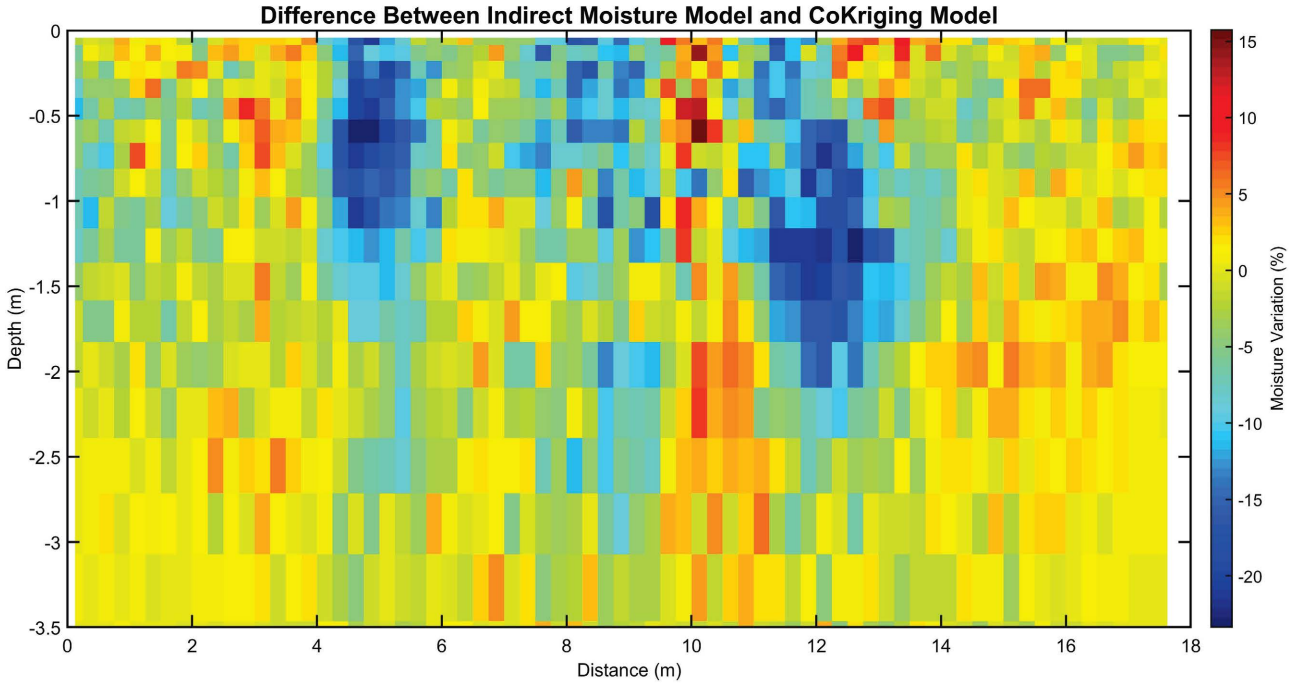

Figure 7. Model of the difference between the soil moisture model obtained from electrical resistivity and the model obtained with Cokriging.

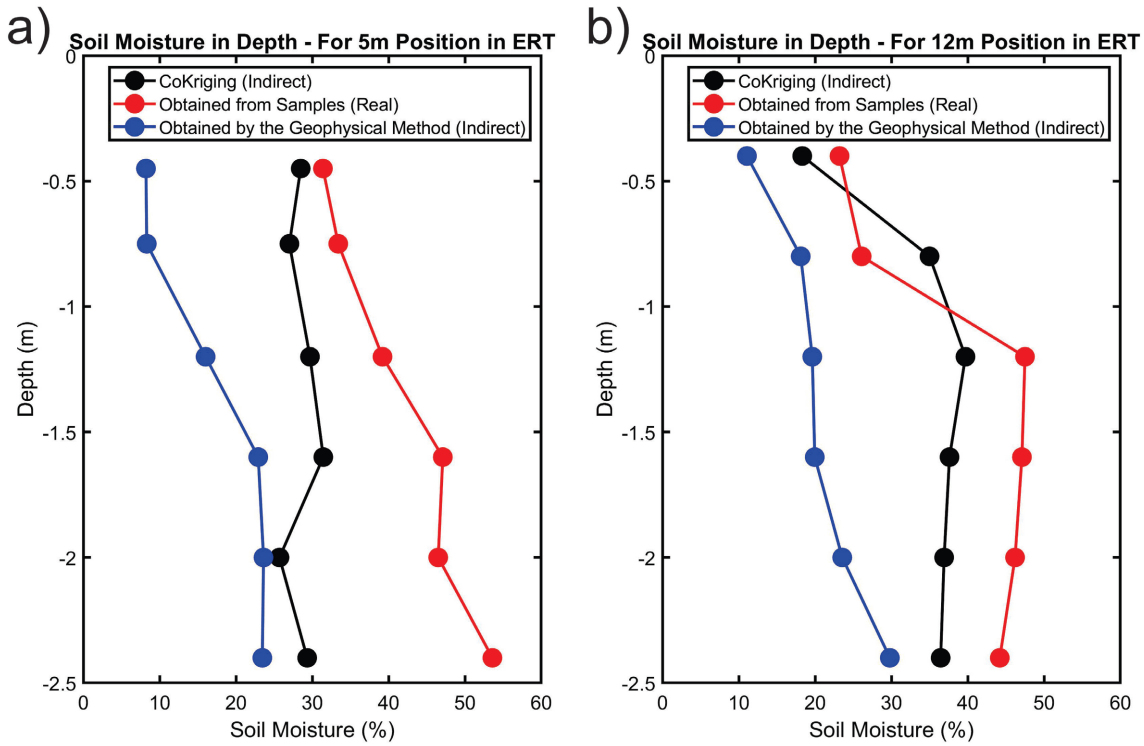

Figure 8. Moisture values at positions 5 m (a) and 12 m (b) of the geophysical profile. In red the values obtained with the samples (direct data), in blue the values obtained indirectly through the resistivity model and in black the values obtained with Cokriging.

Conversely, the moisture values estimated through Cokriging exhibit a closer approximation to the sample values while maintaining characteristics reflective of the primary model. This suggests that the Cokriging methodology effectively integrates the geophysical and geotechnical data to enhance the accuracy of moisture estimations.

Figure 9 extends this comparative analysis by comparing the moisture values obtained from samples, the PCD, and the indirect calculations. The data from the PCD were not used in the Cokriging process but are included here to demonstrate how the model has been refined. The results indicate that the moisture values in the model obtained through Cokriging align more closely with those from the PCD compared to the primary model.

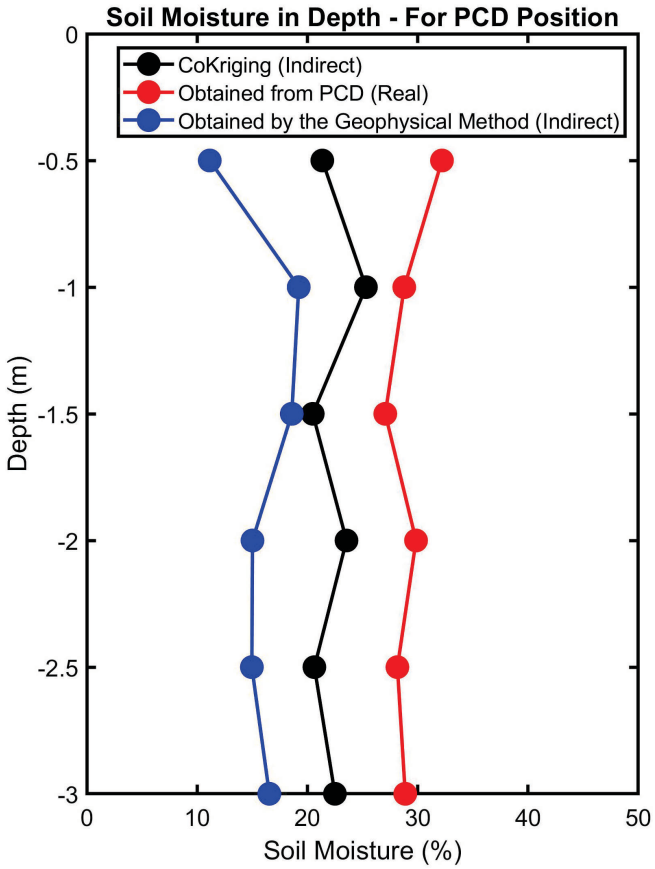

Figure 9. Moisture values at the 9 m position of the geophysical profile, at the PCD installation location. In red the values obtained with PCD (direct data), in blue the values obtained indirectly through the resistivity model and in black the values obtained with Cokriging.

5.4. Cokriging Interpolation - ERT Profile and Plasticity Index

The procedure for indirect calculation was similarly applied to the plasticity index using formulas from [24], as shown in Figure 10. In locations with buried pipes and debris previously described, the plasticity index values are close to or below zero. This suggests that the applied formula for determining this property is not suitable for areas with anthropogenic structures.

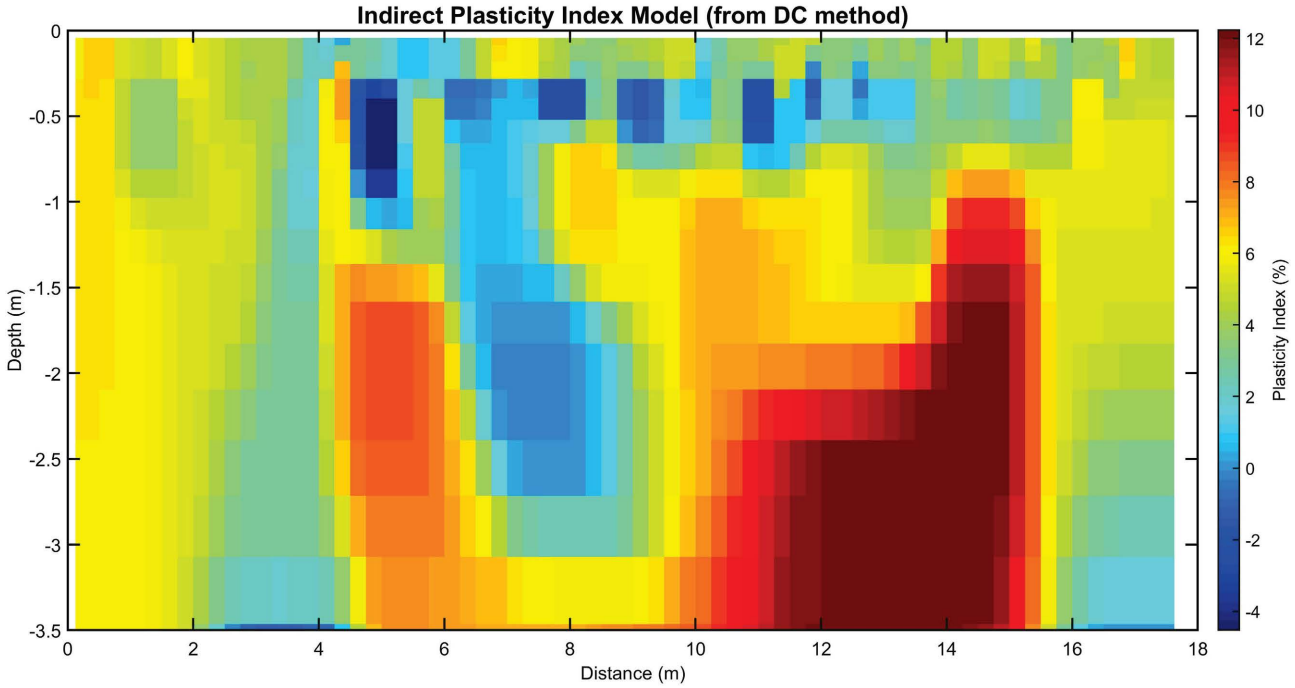

Figure 10. Primary data for plasticity index Cokriging. Plasticity Index model obtained indirectly from the resistivity model.

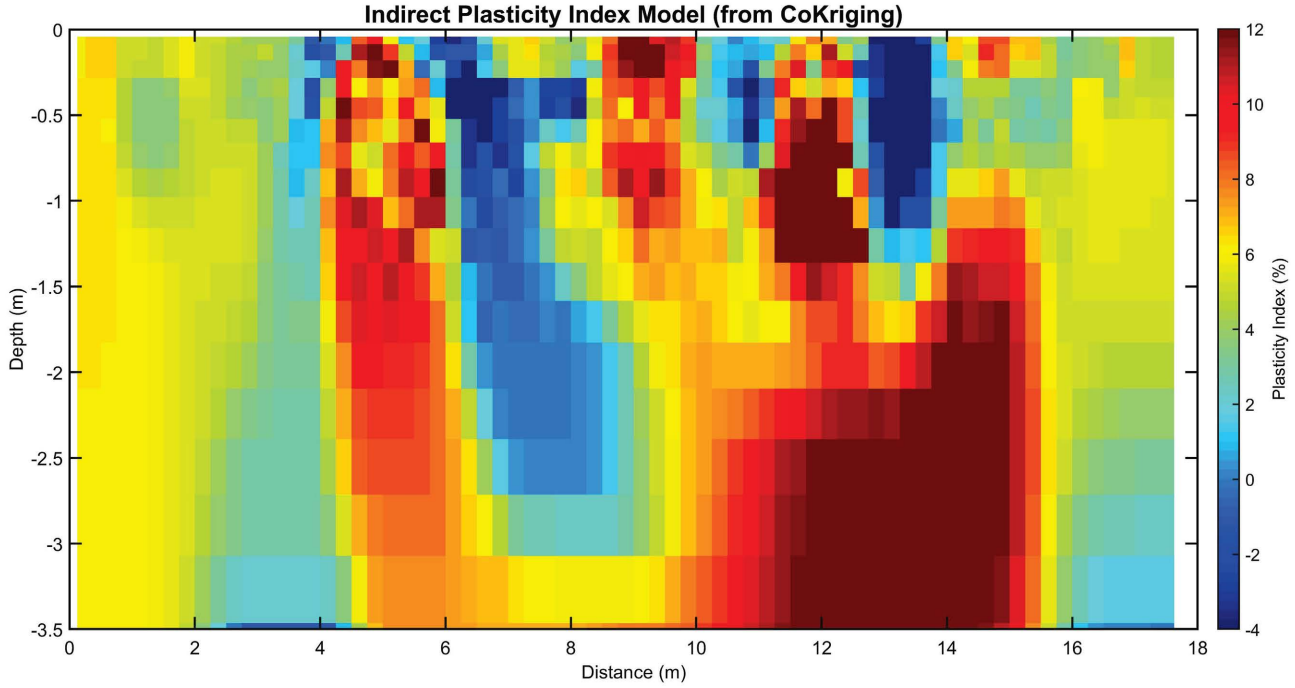

Figure 11. The plasticity Index model was obtained with the Cokriging algorithm.

Figure 11 displays the plasticity index model refined through the Cokriging methodology. This approach significantly reduced the occurrence of anomalies with plasticity index values close to or below zero, effectively eliminating most of the smaller anomalies while accentuating the larger ones. The comparative analysis of both models is illustrated in Figure 12, highlighting that the most signif-

icant variations between the two models occur at positions where shallow anomalies near a depth of 0.5 m were initially detected.

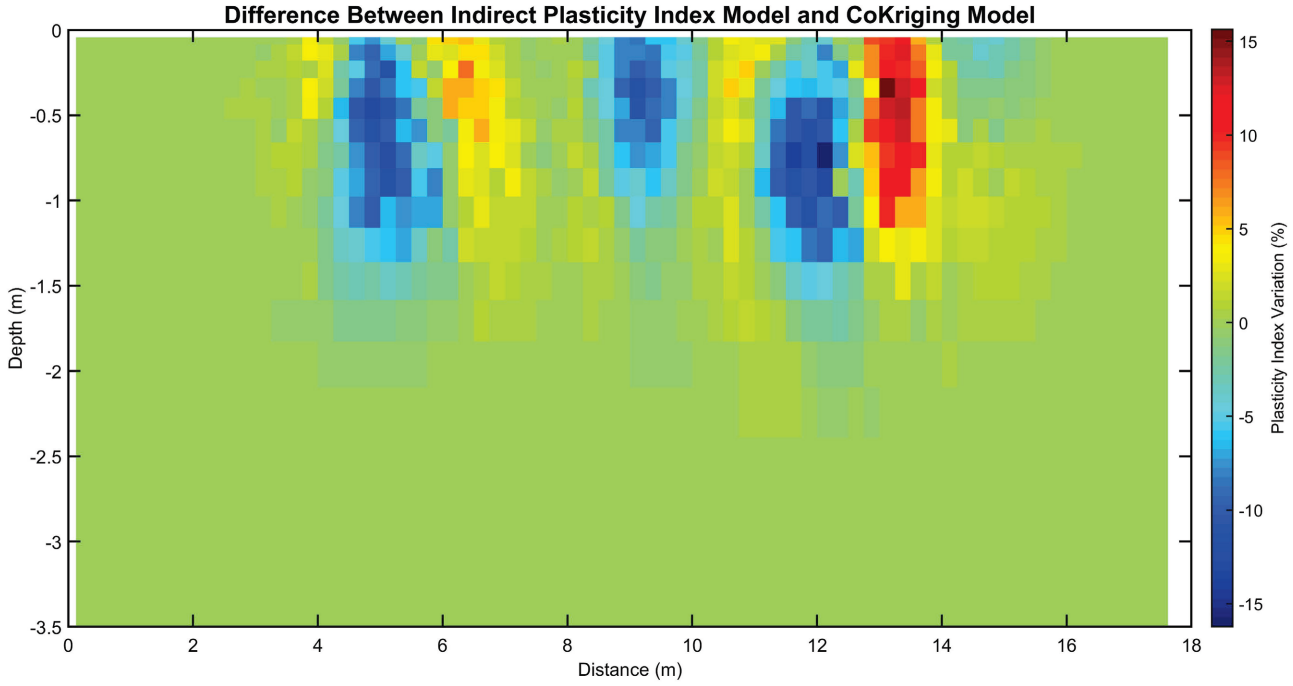

Figure 12. Model of the difference between the plasticity index model obtained from electrical resistivity and the model obtained with Cokriging

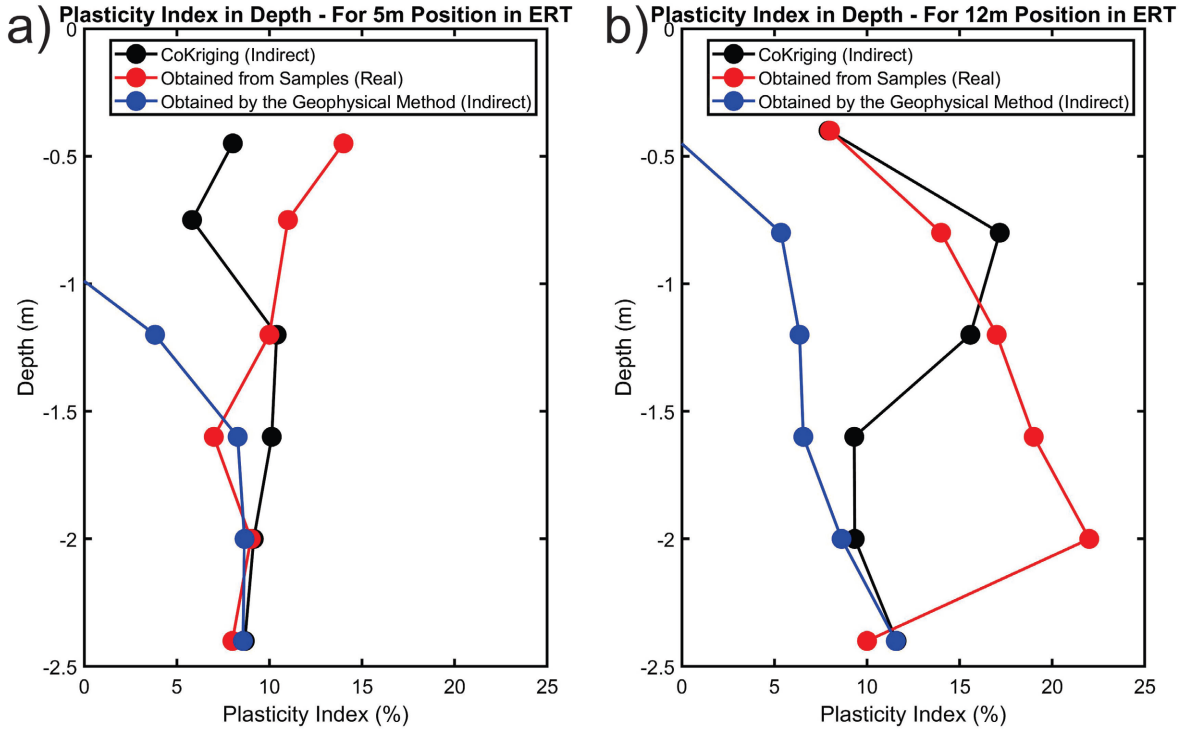

Figure 13. Plasticity Index values at positions 5 m (a) and 12 m (b) of the geophysical profile. In red the values obtained with the samples (direct data), in blue the values obtained indirectly through the resistivity model and in black the values obtained with Cokriging.

Figure 13(a) and Figure 13(b) display the plasticity index values at the 5 m and 12 m positions of the geophysical profile, respectively, obtained from direct sampling, indirect calculations from the resistivity model, and through the Cokriging methodology. These figures demonstrate an overall improvement in the plasticity index values across both locations.

At the 5 m position, the primary model initially reported negative plasticity index values for the first two measurements and a very low value for the third. The application of Cokriging significantly adjusted these values to align more closely with those obtained from direct samples, illustrating a marked improvement in the model's accuracy. Similarly, at the 12 m position, the first point also initially showed a negative value in the primary model. After applying Cokriging, this value was adjusted to more closely approximate the directly measured sample value.

6. Conclusions

This study has established a methodology that combines the electrical resistivity method with traditional geotechnical sampling to create enhanced geotechnical models. The integration of geophysical and geotechnical data through Cokriging offers a nuanced visualization of subsurface conditions, thereby deepening our understanding of soil behavior, which is essential for accurate landslide risk assessments.

By bridging the gap between point-specific data obtained from direct sampling and the broader insights provided by geophysical methods, this approach allows for a comprehensive analysis of subsurface conditions. This is crucial for engineers and planners in making informed decisions that enhance safety and mitigate risks in slope stability assessments and other civil engineering applications.

The Cokriging methodology, in particular, has proven effective in reconciling the discrepancies between direct sample data and the resistivity-derived models. It addresses the limitations posed by traditional indirect methods, especially in areas affected by anthropogenic changes such as construction and utility installations. Through this integration, both the soil moisture and plasticity index models saw substantial improvements in accuracy, demonstrating the methodology's capability to refine data interpretation and reduce the anomalies associated with isolated methods.

The success of this study suggests that the fusion of geophysical imaging with precise geotechnical data via Cokriging not only enhances the detail and reliability of geotechnical models but also elevates the overall efficacy of geological assessments. This innovative approach promises significant advancements in the field of geotechnical engineering, particularly in the management and analysis of complex subsurface environments.

Acknowledgements

Cassiano Bortolozo thanks to the Conselho Nacional de Desenvolvimento

Científico e Tecnológico (CNPq) for the Postdoc-toral Scholarship (grant 152269/2022-3), for the Research Fellowship Program (grant 301201/2022-6) and also for the Re-search Financial Support (Universal Project grant 433481/2018-8). Tristan Pryer and Noel Howley are grateful to the Institute for Mathematical Innovation for supporting this work. All authors thank FINEP (Financiadora de Estudos e Projetos) for financing the REDEGEO project (Carta Convite MCTI/FINEP/FNDCT 01/2016), responsible for the PCD network installation.

Conflicts of Interest

The authors declare no conflicts of interest regarding the publication of this paper.

References

[1] IPCC: Intergovernmental Panel on Climate Change (2021) Climate Change 2021: The Physical Science Basis. Contribution of Working Group I to the Sixth Assessment Report of the Intergovernmental Panel on Climate Change. Cambridge University Press.

[2] de Souza, D.C., Crespo, N.M., da Silva, D.V., Harada, L.M., de Godoy, R.M.P., Domingues, L.M., *et al.* (2024) Extreme Rainfall and Landslides as a Response to Human-Induced Climate Change: A Case Study at Baixada Santista, Brazil, 2020. *Natural Hazards*. https://doi.org/10.1007/s11069-024-06621-1

[3] IBGE: Instituto Brasileiro de Geografia e Estatística (2014) AGÊNCIA IBGE NOTÍCIAS MUNIC 2013: Enchentes deixaram 1, 4 milhão de desabrigados ou desalojados entre 2008 e 2012. https://agenciadenoticias.ibge.gov.br/agencia-sala-de-imprensa/2013-agencia-de-noti-cias/releases/14601-asi-munic-2013-enchentes-deixaram-14-milhao-de-desabrigados-ou-desalojados-entre-2008-e-2012

[4] UFSC-CEPED: Universidade Federal de Santa Catarina and Centro Universitário de Estudos e Pesquisas sobre Desastres (2012) Atlas brasileiro de desastres naturais 1991 a 2010: Volume Brasil.

[5] OPAS (2014) Proteger a saúde frente à mudança climática: Avaliação da vulnerabilidade e adaptação.

[6] Bini, L.M. and Azevedo, T.R. (2014) Vulnerabilidade socioambiental e risco de desastres em áreas de encosta: Análise do evento de 2011 na Região Serrana do Rio de Janeiro. *Geografias*, **10**, 48-67.

[7] Andrade, M.R.M.D., Bortolozo, C.A., Carvalho, A.R., Egas, H.M., Garcia, K., Metodiev, D., *et al.* (2023) The SNAKE System: Cemaden's Landslide Early Warning System (LEWS) Mechanism. *International Journal of Geosciences*, **14**, 1146-1159. https://doi.org/10.4236/ijg.2023.1411058

[8] Moraes, M.V.D., Pampuch, L.A., Bortolozo, C.A., Mendes, T.S.G., Andrade, M.R.M.D., Metodiev, D., *et al.* (2023) Thresholds of Instability: Precipitation, Landslides, and Early Warning Systems in Brazil. *International Journal of Geosciences*, **14**, 895-912. https://doi.org/10.4236/ijg.2023.1410048

[9] Metodiev, D., Andrade, M.R.M.D., Mendes, R.M., Moraes, M.A.E.D., Konig, T.,

Bortolozo, C.A., *et al.* (2018) Correlation between Rainfall and Mass Movements in North Coast Region of Sao Paulo State, Brazil for 2014-2018. *International Journal of Geosciences*, **9**, 669-679. https://doi.org/10.4236/ijg.2018.912040

[10] Bortolozo, C.A., Andrade, M.R.M., Mendes, R.M., Mendes, T.S.G., Motta, M.F.B., Lavalle, L.V.A., Simoes, S.J.C., Pampuch, L.A., Pryer, T., Legg, A., Ashby, B., Renk, J. and Metodiev, D. (2021) How DC and FDEM Methods Can Help Reconstruct the 90-Year History of Occupation of an Urban Area in Campos do Jordão, São Paulo-Brazil and Their Applications in Mass Movement Studies. *AGU Fall Meeting* 2021, New Orleans, 13-17 December 2021,1 p.

[11] Bortolozo, C.A., Pampuch, L.A., Andrade, M.R.M.D., Metodiev, D., Carvalho, A.R., Mendes, T.S.G., *et al.* (2024) ARHCS (Automatic Rainfall Half-Life Cluster System): A Landslides Early Warning System (LEWS) Using Cluster Analysis and Automatic Threshold Definition. *International Journal of Geosciences*, **15**, 54-69. https://doi.org/10.4236/ijg.2024.151005

[12] Sousa, I.A., Bortolozo, C.A., Gonçalves Mendes, T.S., de Andrade, M.R.M., Neto, G.D., Metodiev, D., *et al.* (2023) Development of a Soil Moisture Forecasting Method for a Landslide Early Warning System (LEWS): Pilot Cases in Coastal Regions of Brazil. *Journal of South American Earth Sciences*, **131**, Article ID: 104631. https://doi.org/10.1016/j.jsames.2023.104631

[13] Bortolozo, C.A., Souza, I.A., Andrade, M.R.M., Mendes, T.S.G., Dolif, G., Pryer, T., Simões, S.J.C., Mendes, R.M. and Metodiev, D. (2022) The Development of a Landslide Alert System Based on the Prediction of Soil Moisture in Critical Cities in Brazil-Preliminary Results with the Cemaden's Observation Network. *The AGU* 2022 *Fall Meeting*, Chicago, 12-16 December 2022, NH42C-0437.

[14] Bortolozo, C.A., Mendes, T.S.G., Metodiev, D., Moraes, M.V.D., Egas, H.M., Andrade, M.R.M.D., *et al.* (2024) A Novel Simulator for Probing Water Infiltration in Rain-Triggered Landslides. *First Break*, **42**, 37-43. https://doi.org/10.3997/1365-2397.fb2024054

[15] Bortolozo, C.A., Mendes, T.S.G., Egas, H.M., Metodiev, D., Moraes, M.V.D., Andrade, M.R.M.D., *et al.* (2023) Enhancing Landslide Predictability: Validating Geophysical Surveys for Soil Moisture Detection in 2D and 3D Scenarios. *Journal of South American Earth Sciences*, **132**, Article ID: 104664. https://doi.org/10.1016/j.jsames.2023.104664

[16] Khan, M.A., Basharat, M., Riaz, M.T., Sarfraz, Y., Farooq, M., Khan, A.Y., *et al.* (2021) An Integrated Geotechnical and Geophysical Investigation of a Catastrophic Landslide in the Northeast Himalayas of Pakistan. *Geological Journal*, **56**, 4760-4778. https://doi.org/10.1002/gj.4209

[17] Pasierb, B., Grodecki, M. and Gwóźdź, R. (2019) Geophysical and Geotechnical Approach to a Landslide Stability Assessment: A Case Study. *Acta Geophysica*, **67**, 1823-1834. https://doi.org/10.1007/s11600-019-00338-7

[18] Mezerreg, N.E.H., Kessasra, F., Bouftouha, Y., Bouabdallah, H., Bollot, N., Baghdad, A., *et al.* (2019) Integrated Geotechnical and Geophysical Investigations in a Landslide Site at Jijel, Algeria. *Journal of African Earth Sciences*, **160**, Article ID: 103633. https://doi.org/10.1016/j.jafrearsci.2019.103633

[19] Bortolozo, C.A., Motta, M.F.B., Andrade, M.R.M.D., Lavalle, L.V.A., Mendes, R.M., Simões, S.J.C., *et al.* (2019) Combined Analysis of Electrical and Electromagnetic Methods with Geotechnical Soundings and Soil Characterization as Applied to a Landslide Study in Campos Do Jordão City, Brazil. *Journal of Applied Geophysics*, **161**, 1-14. https://doi.org/10.1016/j.jappgeo.2018.11.017

[20] Pouyon D.E., Ganno, S. and Tabod C.T. (2012) Geophysical and Geotechnical Investigations of a Landslide in Kekem Area, Western Cameroon. *International Journal of Geosciences*, **3**, 780-789.

[21] Bortolozo, C.A., Andrade, M.R.M., Mendes, T.S.G., Egas, H.M., Moraes, M.A.E., Pryer, T., Prieto, C.C., Metodiev, D., Simoes, S.J.C. and Mendes, R.M. (2022) The Tragedy of Morro do Centenário in Petrópolis-RJ, Brazil (February 15, 2022): Landslide Complexity Analyzed from a Multidisciplinary Perspective. *The AGU* 2022 *Fall Meeting*, Chicago, 12-16 December 2022, NH15B-07.

[22] Bortolozo, C.A., Mendes, T.S.G., Motta, M.F.B., Simões, S.J.C., Pryer, T., Metodiev, D., *et al.* (2023) Obtaining 2D Soil Resistance Profiles from the Integration of Electrical Resistivity Data and Standard Penetration Test (SPT) and Light Dynamic Penetrometer (DPL) Resistance Tests—Applications in Mass Movements Studies. *International Journal of Geosciences*, **14**, 840-854. https://doi.org/10.4236/ijg.2023.149045

[23] Bortolozo, C.A., Simões, S.J.C., Andrade, M.R.M., Mendes, R.M., Lavalle, L.V.A., Motta, M.F.B., Metodiev, D. and Mendes, T.S.G. (2019) Guara Registro de Software—Número do Pedido: BR 51 2019 002544-0. *Revista da Propriedade Industrial*, **2549**, 15.

[24] Siddiqui, F.I. and Osman, S.B.A.B.S. (2012) Simple and Multiple Regression Models for Relationship between Electrical Resistivity and Various Soil Properties for Soil Characterization. *Environmental Earth Sciences*, **70**, 259-267. https://doi.org/10.1007/s12665-012-2122-0

[25] Braga, A.C.O. (2016) Geofísica aplicada: Métodos geoelétricos em hidrogeologia. Oficina de Textos.

[26] Lavalle, L.V.A., Bortolozo, C.A., Moraes, M.A.E., Andrade, M.R.M., Motta, M.F.B., Carvalho, P.E.P. and Mendes, R.M. (2017) SOLAM. Registro de Software—Número do Pedido: BR 51 2017 001354-3. *Revista da Propriedade Industrial*, **2442**, 18.

[27] Brom, A. and Natonik, A. (2017) Estimation of Geotechnical Parameters on the Basis of Geophysical Methods and Geostatistics. *Contemporary Trends in Geoscience*, **6**, 70-79. https://doi.org/10.1515/ctg-2017-0006

[28] Kay, M. and Dimitrakopoulos, R. (2000) Integrated Interpolation Methods for Geophysical Data: Applications to Mineral Exploration. *Natural Resources Research*, **9**, 53-64. https://doi.org/10.1023/a:1010161813931

[29] Mendes, R.M., de Andrade, M.R.M., Tomasella, J., de Moraes, M.A.E. and Scofield, G.B. (2018) Understanding Shallow Landslides in Campos Do Jordão Municipality—Brazil: Disentangling the Anthropic Effects from Natural Causes in the Disaster of 2000. *Natural Hazards and Earth System Sciences*, **18**, 15-30. https://doi.org/10.5194/nhess-18-15-2018

[30] Bortolozo, C.A., Mendes, T.S.G., Motta, M.F.B., Andrade, M.R.M., Lavalle, L.V.A., Mendes, R.M., Simoes, S.J.C. and Metodiev, D. (2021) Geofísica Aplicada em Estudos de Movimentos de Massa e Engenharia de Pequeno Porte. *Boletim SBGf*, **116**, 14-17.

[31] Moraes, M.A.E.D., Filho, W.M.M., Mendes, R.M., Bortolozo, C.A., Metodiev, D., Andrade, M.R.M.D., *et al.* (2024) Antecedent Precipitation Index to Estimate Soil Moisture and Correlate as a Triggering Process in the Occurrence of Landslides. *International Journal of Geosciences*, **15**, 70-86. https://doi.org/10.4236/ijg.2024.151006

[32] Bortolozo, C.A., Lavalle, L.V.A., de Andrade, M.R.M., Motta, M.F.B., Mendes, R.M., Metodiev, D., *et al.* (2018) Geophysical Methods to Characterize a Mass Movement

Event in Tropical Soils in Campos Do Jordão City, Brazil. *First Break*, **36**, 71-73. https://doi.org/10.3997/1365-2397.n0115

[33] Lavalle, L.V.A., Bortolozo, C.A., Pacheco, T.C.K.F., de Andrade, M.R.M., Motta, M.F.B., Mendes, R.M., *et al.* (2018) Evaluation Methodology for Obtaining Geotechnical Parameters Using Electrical Resistivity. *First Break*, **36**, 55-58. https://doi.org/10.3997/1365-2397.n0112

[34] Trouw, C.C., Medeiros, F.F.F.d. and Trouw, R.A.J. (2007) Evolução tectônica da Zona de Cisalhamento Caxambu, MG. *Revista Brasileira de Geociências*, **37**, 767-776. https://doi.org/10.25249/0375-7536.2007374767776

[35] Almeida, F.F.M. (1976) The System of Continental Rifts Bordering the Santos Basin, Brazil. *Anais Academia Brasileira de Ciências*, **48**, 15-26.

[36] Serviço Geológico do Brasil (CPRM) (2007) Relatório Anual 2007. https://rigeo.cprm.gov.br/jspui/handle/doc/14644

[37] Ashby, B., Bortolozo, C., Lukyanov, A. and Pryer, T. (2021) Adaptive Modelling of Variably Saturated Seepage Problems. *The Quarterly Journal of Mechanics and Applied Mathematics*, **74**, 55-81. https://doi.org/10.1093/qjmam/hbab001

[38] Leite, D.N., Bortolozo, C.A., Porsani, J.L., Couto, M.A., Campaña, J.D.R., dos Santos, F.A.M., *et al.* (2018) Geoelectrical Characterization with 1D VES/TDEM Joint Inversion in Urupês-Sp Region, Paraná Basin: Applications to Hydrogeology. *Journal of Applied Geophysics*, **151**, 205-220. https://doi.org/10.1016/j.jappgeo.2018.02.022

[39] Hamada, L.R., Porsani, J.L., Bortolozo, C.A. and Rangel, R.C. (2018) TDEM and VES Soundings Applied to a Hydrogeological Study in the Central Region of the Taubaté Basin, Brazil. *First Break*, **36**, 49-54. https://doi.org/10.3997/1365-2397.n0111

[40] Rangel, R.C., Porsani, J.L., Bortolozo, C.A. and Hamada, L.R. (2018) Electrical Resistivity Tomography and TDEM Applied to Hydrogeological Study in Taubaté Basin, Brazil. *International Journal of Geosciences*, **9**, 119-130. https://doi.org/10.4236/ijg.2018.92008

[41] Bortolozo, C.A., Campaña, J.D.R., Junior, M.A.C., Porsani, J.L. and dos Santos, F.A.M. (2016) The Effects of Negative Values of Apparent Resistivity in TEM Surveys. *International Journal of Geosciences*, **7**, 1182-1190. https://doi.org/10.4236/ijg.2016.710088

[42] Bortolozo, C.A., Couto, M.A., Porsani, J.L., Almeida, E.R. and Monteiro dos Santos, F.A. (2014) Geoelectrical Characterization Using Joint Inversion of VES/TEM Data: A Case Study in Paraná Sedimentary Basin, São Paulo State, Brazil. *Journal of Applied Geophysics*, **111**, 33-46. https://doi.org/10.1016/j.jappgeo.2014.09.009

[43] Telford, W.M., Geldart, L.P. and Sheriff, R.E. (1990) Applied Geophysics. 2nd Edition, Cambridge University Press. https://doi.org/10.1017/cbo9781139167932

[44] Xavier, F.F. (2010) Geofísica Elétrica aplicada a Geotecnia para investigação de estabilidade de taludes. Tecgeofisica, Florianópolis, Santa Catarina, Brasil.

[45] Godio, A. and Bottino, G. (2001) Electrical and Electromagnetic Investigation for Landslide Characterisation. *Physics and Chemistry of the Earth, Part C: Solar, Terrestrial & Planetary Science*, **26**, 705-710. https://doi.org/10.1016/s1464-1917(01)00070-8

[46] Schmutz, M., Albouy, Y., Guérin, R., Maquaire, O., Vassal, J., Schott, J., *et al.* (2000) Joint Electrical and Time Domain Electromagnetism (TDEM) Data Inversion Applied to the Super Sauze Earthflow (France). *Surveys in Geophysics*, **21**, 371-390.

https://doi.org/10.1023/a:1006741024983

[47] Schmutz, M., Guérin, R., Andrieux, P. and Maquaire, O. (2009) Determination of the 3D Structure of an Earthflow by Geophysical Methods: The Case of Super Sauze, in the French Southern Alps. *Journal of Applied Geophysics*, **68**, 500-507. https://doi.org/10.1016/j.jappgeo.2008.12.004

[48] Perrone, A., Lapenna, V. and Piscitelli, S. (2014) Electrical Resistivity Tomography Technique for Landslide Investigation: A Review. *Earth-Science Reviews*, **135**, 65-82. https://doi.org/10.1016/j.earscirev.2014.04.002

[49] Koefoed, O. (1972) A Note on the Linear Filter Method of Interpreting Resistivity Sounding Data. *Geophysical Prospecting*, **20**, 403-405. https://doi.org/10.1111/j.1365-2478.1972.tb00643.x

[50] Andrade, M.R.M., Bortolozo, C.A., Mendes, R.M., Metodiev, D., Moraes, M.A.E., Renk, J., Mendes, T.S.G. and Simoes, S.J.C. (2021) Challenges in Implementing a landslide Warning System Based on Soil Moisture Sensors in a Continental-Sized Country Like Brazil-Preliminary Results. *AGU Fall Meeting* 2021, New Orleans, 13-17 December 2021, 1 p.